A Mathematical Model of Electrotonic Interactions between Ventricular Myocytes and Fibroblasts

K. Andrew MacCannell,* Hojjat Bazzazi,* Lisa Chilton,* Yoshiyuki Shibukawa,* Robert B. Clark,* and Wayne R. Giles*†

*Department of Physiology and Biophysics, Faculty of Medicine, University of Calgary, Calgary, Alberta, Canada; and †Faculty of Kinesiology, University of Calgary, Calgary, Alberta, Canada

ABSTRACT Functional intercellular coupling has been demonstrated among networks of cardiac fibroblasts, as well as between fibroblasts and atrial or ventricular myocytes. In this study, the consequences of these interactions were examined by implementing the ten Tusscher model of the human ventricular action potential, and coupling it to our electrophysiological models for mammalian ventricular fibroblasts. Our simulations reveal significant electrophysiological consequences of coupling between 1 and 4 fibroblasts to a single ventricular myocyte. These include alterations in plateau height and/or action potential duration (APD) and changes in underlying ionic currents. Two series of simulations were carried out. First, fibroblasts were modeled as a spherical cell with a capacitance of 6.3 pF and an ohmic membrane resistance of 10.7 GΩ. When these "passive" fibroblasts were coupled to a myocyte, they caused slight prolongation of APD with no changes in the plateau, threshold for firing, or rate of initial depolarization. In contrast, when the same myocyte-fibroblast complexes were modeled after addition of the time- and voltage-gated K^+ currents that are expressed in fibroblasts, much more pronounced effects were observed: the plateau height of the action potential was reduced and the APD shortened significantly. In addition, each fibroblast exhibited significant electrotonic depolarizations in response to each myocyte action potential and the resting potential of the fibroblasts closely approximated the resting potential of the coupled ventricular myocyte.

INTRODUCTION

Myocytes and fibroblasts are the two major cell types in healthy mammalian ventricular myocardium. Although myocytes are primarily responsible for the mechanical function and occupy most of the tissue volume, fibroblasts outnumber myocytes by ~1.4 to 1 (1). In canine left ventricle, fibroblasts have been identified in the immediate vicinity of each myocyte (2). Furthermore, the gap junction proteins, connexins 43 (Cx43) and 45 (Cx45), are expressed by cardiac fibroblasts, and dye coupling from fibroblasts to atrial and ventricular myocytes has been demonstrated (3,4). These findings suggest that myocytes and fibroblasts are functionally coupled by gap junctions and may interact via two-way electrotonic signaling (5,6).

In an experimental system consisting of cocultured neonatal cardiac myocytes and fibroblasts, spatially defined pairs of myocytes separated by a fibroblast have been shown to communicate via electrotonic signaling. Furthermore, the fibroblasts that were coupled to myocyte(s) exhibited electrotonic changes in membrane potential, and these resembled the myocyte action potential. Cx43 is expressed in these cell cultures (7,8). Recently, these findings and principles have been extended to an important pathophysiological setting. Electrophysiological coupling has been studied between neonatal rat heart myocytes and myofibroblasts plated in culture as either narrow columns of myocytes separated by myofibroblast inserts, or as sheets of myocytes covered with variable numbers of myofibroblasts (9). In both configurations, electrotonic coupling of these two cell types, and propagation of action potentials from myocytes to myofibroblasts were observed. This article also reported that when variable numbers of myofibroblasts were cultured over sheets of neonatal myocytes, recordings from myocytes showed that the rate of action potential depolarization and conduction velocity decreased with increasing density of myofibroblasts. Previous work had shown that mechanosensitive atrial or sinoatrial fibroblasts were also coupled electrotonically to adjacent myocytes (10,11). Thus, electrotonic coupling can occur in vivo as well as in culture.

In this theoretical study, the consequences of this electrotonic coupling are explored by developing a mathematical model that can account for the main functional components responsible for this coupling between adult cardiac fibroblasts and myocytes. We have recently identified inwardly-rectifying (K_{ir}), and time- and voltage-gated (K_v) K^+ currents in fibroblasts and myofibroblasts from adult rat ventricular tissue (12,13). A mathematical model of the electrophysiological properties of adult ventricular fibroblast was developed and then integrated with the ten Tusscher model of the human ventricular myocyte (14). Linear resistive coupling was chosen as the basis for intercellular electrotonic interactions. These parameters were based on the known

Submitted November 19, 2006, and accepted for publication December 28, 2006.

Address reprint requests to Dr. Wayne R. Giles, Faculty of Kinesiology, University of Calgary, Calgary, AB, Canada T2N 4N1. Tel.: 403-220-5607; Fax: 403-220-0448; E-mail: wgiles@ucalgary.ca.

Y. Shibukawa's present address is Dept. of Physiology, Tokyo Dental College, Chiba 261-8502, Japan; H. Bazzazi's present address is Dept. of Bioengineering, Johns Hopkins University, Baltimore, MD 21205.

© 2007 by the Biophysical Society

0006-3495/07/06/4121/12 $2.00

doi: 10.1529/biophysj.106.101410

properties of connexin isoforms, that are expressed in mammalian ventricle. The physiological effects of this cell-cell interaction were then investigated and related to available microanatomical and physiological data. This was done by selective alterations in 1), the ratio of myocytes to fibroblasts; and 2), the values of intercellular resistance. Specifically, we simulated electrotonic interactions between one myocyte and one to four fibroblasts, where the fibroblast was modeled 1), as a passive R-C circuit, and then 2), with the K_{ir} and K_v currents that are expressed in the fibroblast. The coupling resistance varied between 1 and 3 nS. When the fibroblast is modeled as a passive R-C circuit, it has little effect on APD or action potential waveform. In contrast, coupling of a ventricular myocyte to fibroblasts in which K_{ir} and K_v currents are included shortened ventricular myocyte APD and reduced the plateau height of the action potential, indicating that coupling of cardiac fibroblasts and myocytes may have significant effects on myocyte electrophysiology. In addition, each myocyte action potential results in significant electrotonic depolarization in each fibroblast, thus raising the possibility that excitation-secretion coupling in the fibroblast may be modulated by myocyte electrophysiological activity.

METHODS

The ten Tusscher model of the human ventricular action potential

The ten Tusscher mathematical model of the human ventricular epicardial myocyte action potential (14) is robust, computationally efficient, and internally consistent. It originates from a previous mathematical formulation of the human ventricular myocyte action potential, the Priebe-Beukelmann model (15), but is based on a broader set of experimental data, much of which was collected in the six years intervening between the publishing of these two models. We note, however, that a number of aspects of this model, e.g., the formulations for the Ca^{2+} current and the equations accounting for Ca^{2+} homeostasis, will need to be modified as new experimental data are published (16).

Cell-cell coupling

In these simulations, a selected number of fibroblasts were resistively coupled to a single myocyte by assigning an intercellular fibroblast-to-myocyte conductance, G_{gap}, which varied between 1 and 3 nS in individual simulations (Fig. 1). This range for G_{gap} covers the approximate values of intercellular conductances reported or derived from measurements on cardiac fibroblasts cocultured with neonatal myocytes (7,9,11). The differential equation for the membrane potential across the cardiac fibroblast membrane is:

$$\frac{dV_{cfi}}{dt} = -\frac{1}{C_{mf}}[I_{cfi}(V_{cfi}, t) + G_{gap}(V_{cfi} - V_{myo})], \qquad (1)$$

where I_{cfi} and V_{cfi} represent the transmembrane current and potential, respectively, across the ith coupled fibroblast; V_{myo} represents the membrane potential across the myocyte cell membrane; C_{mf} represents the fibroblast membrane capacitance (assumed to be constant); and G_{gap} represents the gap-junctional conductance (assumed to be ohmic). A negative I_{gap} (i.e., $G_{gap}(V_{cfi} - V_{myo})$) indicates that current is flowing from the myocyte into the fibroblast.

Similarly, the differential equation for the membrane potential of the myocyte is

$$\frac{dV_{myo}}{dt} = -\frac{1}{C_{mmyo}}\left[I_{myo}(V_{myo}, t) + \sum_{i=1}^{n} G_{gap}(V_{myo} - V_{fi})\right], \qquad (2)$$

where V_{myo} represents the myocyte membrane potential; C_{mmyo} represents the myocyte membrane capacitance; I_{myo} represents the myocyte transmembrane current as defined by the ten Tusscher mathematical model (14); and n is the total number of fibroblasts.

Electrophysiological models of ventricular fibroblasts

Simulations were carried out with two different electrophysiological models of ventricular fibroblasts. The first model consisted of a membrane capacitance and an ohmic resistance connected in parallel. The electrical

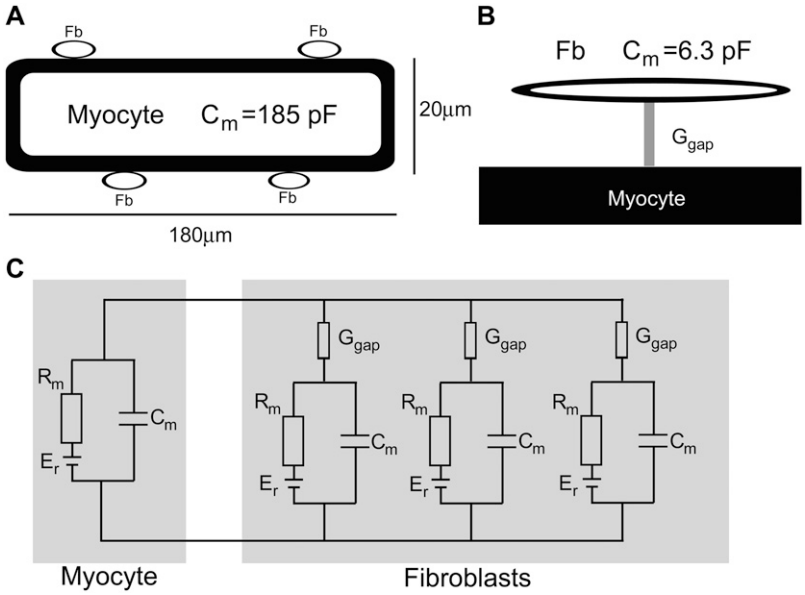

FIGURE 1 Diagram illustrating the paradigm that is the basis for this hybrid mathematical model of the electrotonic interactions between ventricular myocytes and fibroblasts. (*A*) Entire hybrid system: a single human ventricular myocyte is coupled to a selected number of homogeneous fibroblasts via an intercellular conductance that was varied between 1 and 3 nS in different simulations. (*B*) Simplified view of the fibroblast-myocyte coupling. The membrane capacitance of both the myocyte and the fibroblasts are indicated. (*C*) Equivalent circuit of the coupled myocytes and fibroblasts is illustrated. In each case, R_m represents the membrane resistance of an individual cell, C_m is cell capacitance, E_r is electromotive force, and G_{gap} represents the ohmic gap junctional conductance. R_m of the fibroblast was either a constant, ohmic resistance, or consisted of four time- and voltage-dependent membrane conductances, as described in Methods.

parameters in this ''passive'' model of the fibroblast were based on previous work from our laboratory (12). Membrane capacitance in this passive model was 6.3 pF and membrane resistance was 10.7 GΩ. The second, ''active'' model of the fibroblast, which also had a membrane capacitance of 6.3 pF, included four membrane ionic currents, two of which we have identified and characterized in detail in previous studies (12,13). Details of the formulations for the four membrane currents are described below.

Time- and voltage-dependent fibroblast K^+ current (I_{Kv})

A time- and voltage-dependent ''delayed-rectifier'' K^+ current, which is expressed in a large fraction (>70%) of acutely isolated cardiac fibroblasts, has been identified and studied in detail in our laboratory (13). This current has been shown to be sensitive to both TEA and 4-AP (13). Although neither the family nor the isoform of the K^+ channel that is expressed have been identified definitively, the properties of the Kv1 family are consistent with our experimental data, and Kv 1.6 is a likely candidate.

Our experimental results (13) provide a basis for the empirical description of the kinetics of this K^+ current. Our mathematical formulation is based upon the previously published model, from our group, of the time- and voltage-sensitive K^+ current Kv1.5 in human atrium (17). The current, I_{Kv}, is given by the expression

$$I_{Kv} = g_{Kv} r_{Kv} s_{Kv} (V - E_k), \tag{3}$$

where E_k is −87 mV and g_{kv}, the maximum conductance of I_{Kv}, is 0.25 nS/pF. Expressions for r_{Kv} and s_{Kv} are the activation and inactivation parameters, respectively. Initial values of r_{Kv} and s_{Kv} are 0 and 1, respectively. The time dependence is given by

$$\frac{dr_{Kv}}{dt} = \frac{r_{Kv} - \bar{r}}{\tau_r} \tag{4}$$

and

$$\frac{ds_{Kv}}{dt} = \frac{s_{Kv} - \bar{s}}{\tau_s}. \tag{5}$$

The functions describing τ_r and τ_s are voltage-dependent:

$$\tau_r = 20.3 + 138 \exp\left(-\left(\frac{V_f + 20}{25.9}\right)^2\right) \tag{6}$$

and

$$\tau_s = 1574 + 5268 \exp\left(-\left(\frac{V_f + 23.0}{22.7}\right)^2\right). \tag{7}$$

τ_r and τ_s were fitted to the available data presented in Shibukawa et al. (13), using a least-squares procedure.

The steady-state activation and inactivation parameters are given by the following Boltzmann functions:

$$\bar{r} = \frac{1}{1 + \exp\left(-\frac{V_f + 20.0}{11}\right)} \tag{8}$$

and

$$\bar{s} = \frac{1}{1 + \exp\left(\frac{V_f + 23}{7}\right)}. \tag{9}$$

Inward-rectifying K^+ current (I_{K1}) in the fibroblast

The majority of fibroblasts from the ventricles of adult rats express an inwardly-rectifying K^+ current, I_{K1} (12). The Kir2.1 isoform of inwardly-rectifying K^+ channels is highly expressed in cardiac myofibroblasts (12), suggesting that I_{K1} in acutely isolated cardiac fibroblasts may be produced by this K^+ channel isoform. To simulate this K^+ current, the ten Tusscher et al. (14) equation for this nonlinear inward-rectifying K^+ current was scaled to approximate the much smaller capacitance of the cardiac fibroblast. This formulation is as follows:

$$I_{K1} = \frac{g_{K1} \alpha_{K1} (V_f - E_K)}{\alpha_{K1} + \beta_{K1}}, \tag{10}$$

where g_{K1} is the maximal conductance of this inward-rectifying K^+ current. It is assumed to be constant, independent of voltage or time. This quantity was set to a value of 482.2 pS/pF. The functions α_{K1} and β_{K1} are defined as follows:

$$\alpha_{K1} = \frac{0.1}{1 + \exp(0.06(V_f - E_k - 200))} \tag{11}$$

and

$$\beta_{K1} = \frac{3\exp(0.0002(V_f - E_K + 100)) + \exp(0.1(V_f - E_K - 10))}{1 + \exp(-0.5(V_f - E_K))}. \tag{12}$$

Both functions are scalars, representing the fractional open probability of the channels as a function of membrane potential.

Na^+-K^+ pump current (I_{NaK}) in the fibroblast

A Na^+-K^+ pump has not been conclusively identified either in cardiac fibroblasts or myofibroblasts. However, the expression of K^+ channels in the fibroblast and myofibroblast, and resulting K^+ fluxes would seem to require this type of active transport. A Na^+-K^+ pump is universally expressed in mammalian tissues; accordingly, it is logical to conclude that such a pump is also active in cardiac fibroblasts.

The equations for the steady-state current generated by the Na^+-K^+ pump as a function of membrane potential were based on a previous mathematical model developed in this laboratory (17),

$$I_{NaK} = \bar{I}_{NaK} \left(\frac{[K^+]_o}{[K^+]_o + K_{mK}}\right) \left(\frac{[Na^+]_i^{(3/2)}}{[Na^+]_i^{(3/2)} + K_{mNa}^{(3/2)}}\right) \frac{V_f - V_{rev}}{V_f - B}, \tag{13}$$

where V_{rev} is the reversal potential of this electrogenic pump (−150 mV), and B is an empirically determined constant (−200 mV). The value $\bar{I}_{NaK}$ is the maximum current generated, 2.002 pA/pF. K_{mK} and K_{mNa} are binding constants, with values of 1.0 mmol/L and 11.0 mmol/L, respectively.

Background Na^+ current ($I_{b,Na}$) in the fibroblast

A linear background ''leak'' Na^+ conductance was included in the model to balance Na^+ efflux associated with Na^+-K^+ pump activity. The magnitude of this current was adjusted so that Na^+ influx through the leak channel balanced Na^+ efflux via the Na^+-K^+ pump during a cardiac cycle. Na^+ efflux from the fibroblast was determined by integrating the Na^+-K^+ pump current during the cardiac cycle (multiplied by 3, to account for the 3:2 Na^+-K^+ stoichiometry of the Na^+-K^+ pump). The magnitude of the leak conductance was determined by setting the integrated Na^+ influx via the leak pathway equal to the Na^+ efflux via the Na^+-K^+ pump. The background Na^+ current, $I_{b,Na}$, was formulated as:

$$I_{b,Na} = G_{b,Na}\,(V_f - E_{Na}),$$

where the leak conductance $G_{b,Na} = 0.0095$ nS/pF, and E_{Na} is the Nernst potential for Na^+ ions.

The uncoupled, resting membrane potential of the active model of the ventricular fibroblast was −49.6 mV, and membrane slope resistance, measured between −60mV and −80 mV, was 6.9 GΩ.

Simulations were carried out with between one and four identical passive or active fibroblasts coupled to a single ventricular myocyte (Fig. 1) at a constant G_{gap} of 3 nS, or with two coupled fibroblasts in which G_{gap} was varied between 1 and 3 nS. The myocyte was stimulated at 1 Hz with a rectangular current pulse of 1.9 nA and 3 ms duration. To ensure that the simulations were representative of steady-state conditions, 20 stimuli were applied before recording the voltage and membrane currents of the coupled cells.

RESULTS

In this study, the ten Tusscher model (14) of the human epicardial ventricular myocyte action potential was used to investigate the electrophysiological behavior of adult myocytes that were coupled to a selected number of adult cardiac fibroblasts. The mathematical descriptors of both passive and active electrophysiological properties of the ventricular fibroblast have been chosen based upon our experimental data from acutely isolated, adult rat ventricular fibroblasts (12,13).

Effects of passive fibroblasts on ventricular myocyte

Resistive coupling of either 2 or 4 passive fibroblasts to the simulated myocyte with a junctional conductance G_{gap} of 3 nS lengthened the ventricular APD (90% repolarization) from 263 ms (control) to 273 ms or 275 ms, respectively, as shown in Fig. S1 *A* of the Online Supplement. Ventricular myocyte membrane currents I_{K1}, I_{Kr}, and L-type Ca^{2+} current appeared not to be changed significantly by the coupled fibroblasts (Supplementary Material, Fig. S1, *B–D*).

Effects of active fibroblasts on ventricular myocyte

Fig. 2 shows the effects of coupling two or four active fibroblasts to a ventricular myocyte with a G_{gap} of 3 nS. In contrast to the small effects of coupling passive fibroblasts to the ventricular myocyte, active fibroblasts modeled with the four membrane currents, as described in Methods, produced pronounced changes in myocyte action potential waveform (Fig. 2). Repolarization of the ventricular myocyte action potential was accelerated, and the membrane potential during the plateau was less depolarized. These changes depended on the number of coupled fibroblasts (Fig. 2). For example, coupling two or four fibroblasts to a ventricular myocyte via a junctional conductance of 3 nS resulted in a decrease in APD from a control value of 263 ms to 195 and 155 ms, respectively (Fig. 2 *A*). The peak of the action potential was slightly decreased by the coupled fibroblasts (see Supplementary Material, Fig. S2). There was also a small depolarization of the diastolic membrane potential of the myocyte, from −86.1 mV for the uncoupled myocyte to −85.8 mV with two coupled fibroblasts and −85.3 mV with four coupled fibroblasts. A small reduction in the delayed-rectifier K^+ conductance HERG (I_{Kr}) of the myocyte (from 0.50 pA/pF to 0.47 pA/pF with two fibroblasts and 0.40 pA/pF with four fibroblasts coupled with 3-nS conductance) resulted

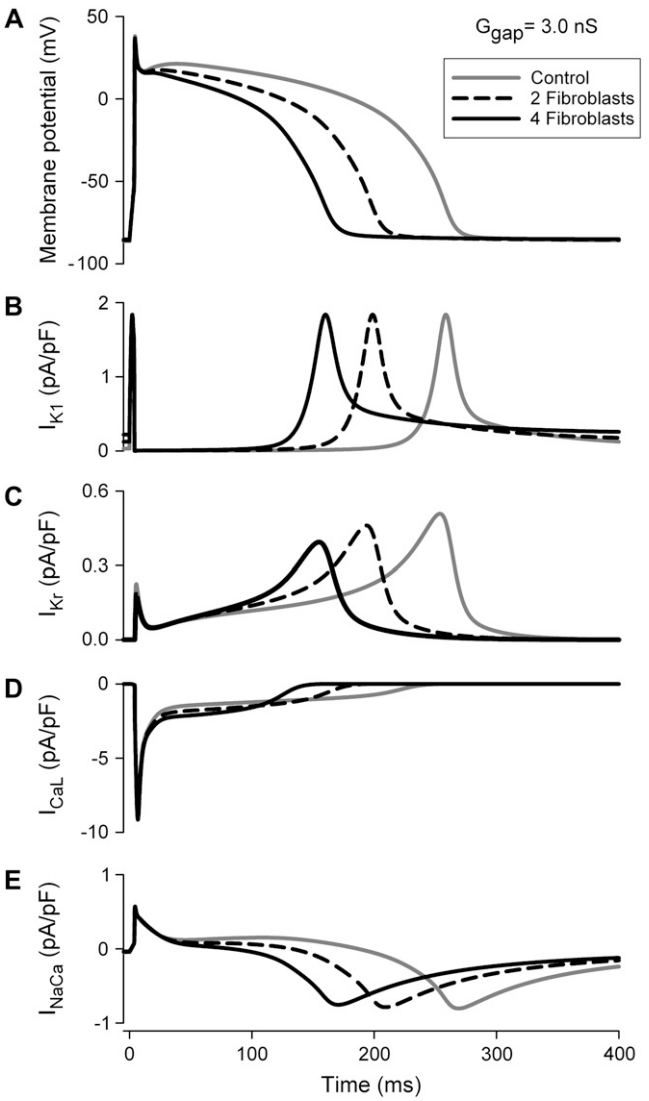

FIGURE 2 Simulations of myocyte-fibroblast interactions under conditions in which the coupled fibroblasts are ''active'', i.e., four membrane currents have been incorporated in the model. (*A*) Changes in myocyte action potential waveform after coupling to two or four fibroblasts via a junctional conductance of 3 nS. (*B–E*) The corresponding changes in myocyte transmembrane currents, where I_{K1} is the inward-rectifying K^+ current, I_{Kr} is the rapidly activating delayed-rectifier (HERG), I_{CaL} is the L-type Ca^{2+} current, and I_{NaCa} is the Na^+-Ca^{2+} exchanger current. Control (uncoupled) myocyte action potential and membrane currents are depicted in gray, the effects of coupling to two fibroblasts are shown with a dashed black line, and changes caused by coupling to four fibroblasts are shown with a solid black line.

from the changes in action potential waveform. Peak Ca^{2+} current in the myocyte increased as a function of fibroblast number from −8.2 pA/pF under control conditions to −8.8 pA/pF (two fibroblasts coupled) and −9.3 pA/pF (four fibroblasts coupled, Fig. 2 *D*), whereas peak inward Na^{+}-Ca^{2+} exchanger current decreased slightly from −0.81 pA/pF to −0.80 or −0.78 pA/pF, when either two or four fibroblasts, respectively, were added. Peak I_{K1} was not changed.

Similar changes in myocyte action potential and membrane currents occurred when the number of coupled fibroblasts was fixed and the junctional conductance was changed. This is shown in Fig. 3, in which two fibroblasts were coupled to a myocyte via a junctional conductance of 1–3 nS. Increasing the junctional conductance resulted in greater reduction in APD. For example, with junctional conductance of 1 or 2 nS, APD was 225 or 207 ms, respectively, compared with the control duration of 263 ms.

Electrotonic changes in fibroblast membrane potential

Given that fibroblasts are coupled by gap junctions to myocytes in vivo (2–4), we were interested in whether, and to what extent, the ventricular action potential can electrotonically modulate fibroblast membrane potential. As shown in Figs. 4 and 5, the action potential of the coupled myocyte produced substantive electrotonic depolarization in the

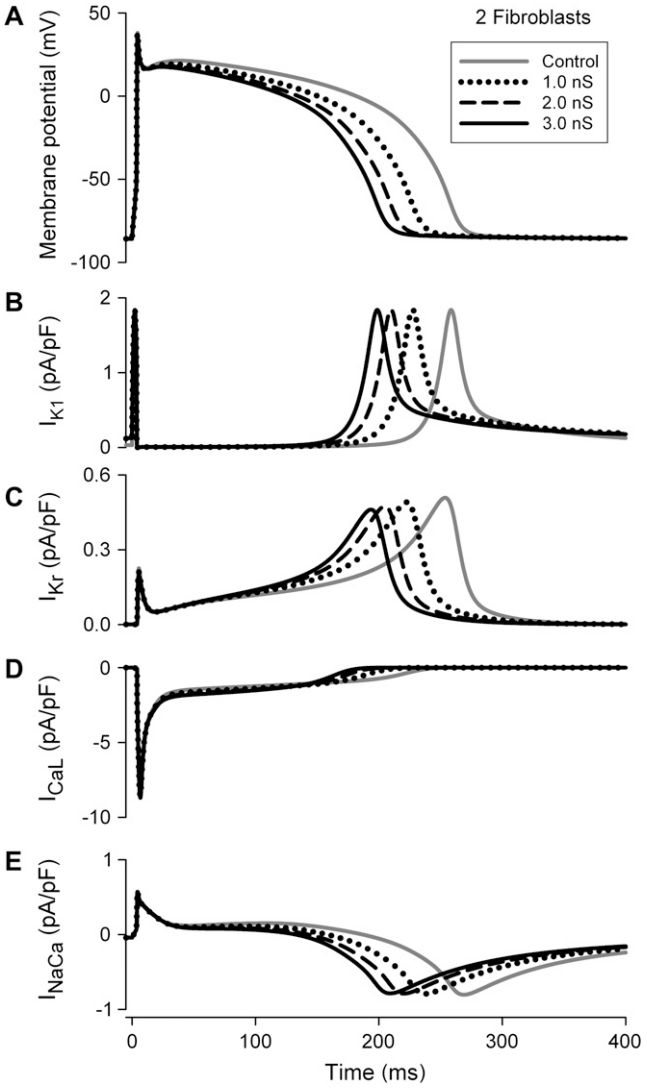

FIGURE 3 Simulation of effects of changing junctional conductance with two active fibroblasts coupled with a ventricular myocyte at selected coupling conductances. Note that the effects on action potential waveform (*A*) and myocyte currents (*B–E*) are more marked with increasing coupling conductance. In each panel, control curves are depicted in gray. Coupling the myocyte to two fibroblasts with a junctional conductance of 1 (*dotted line*), 2 (*dashed line*), or 3 (*solid black line*) nS shortened the APD (*A*). These changes in action potential waveform reduced I_{Kr} (*C*) and shortened L-type Ca^{2+} current duration (*D*). Peak myocyte I_{K1} current (*B*), L-type Ca^{2+} current (*D*), and Na^{+}/Ca^{2+} exchange current were unaffected.

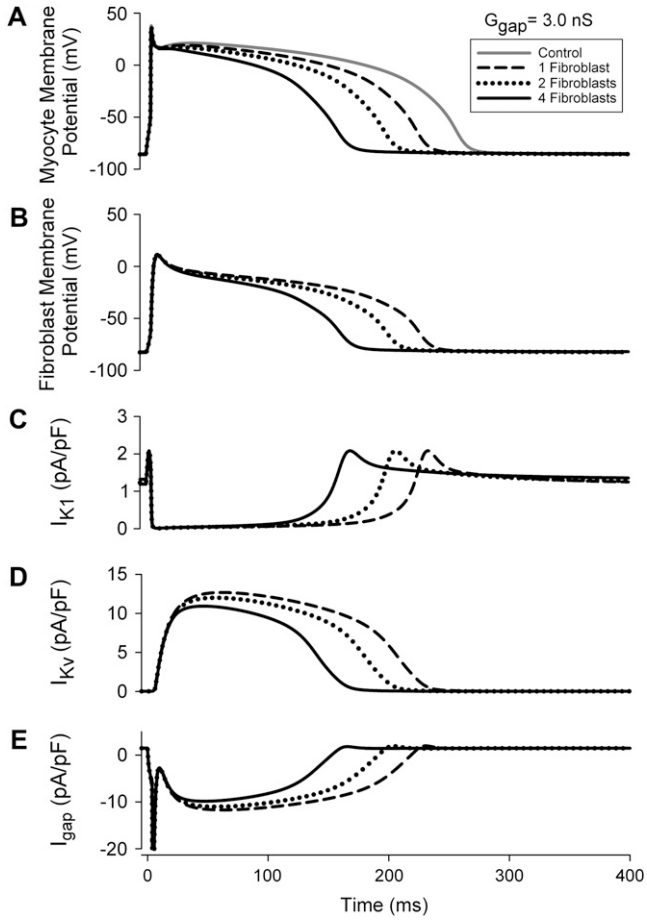

FIGURE 4 Illustration of changes in the waveform of the ventricular action potential (*A*), fibroblast membrane potential (*B*), inwardly-rectifying K^{+} current, I_{K1}, in the fibroblast (*C*), time- and voltage-gated K^{+} current, I_{Kv}, in the fibroblast (*D*), and gap junction current, I_{gap} (*E*), during a ventricular action potential after coupling of the myocyte to one (*dashed line*), two (*dotted line*), or four (*solid black line*) active fibroblasts, via a junctional conductance of 3 nS. The control myocyte action potential is shown as a gray line in *A*. A negative I_{gap} indicates that current is flowing from the myocyte into the fibroblast.

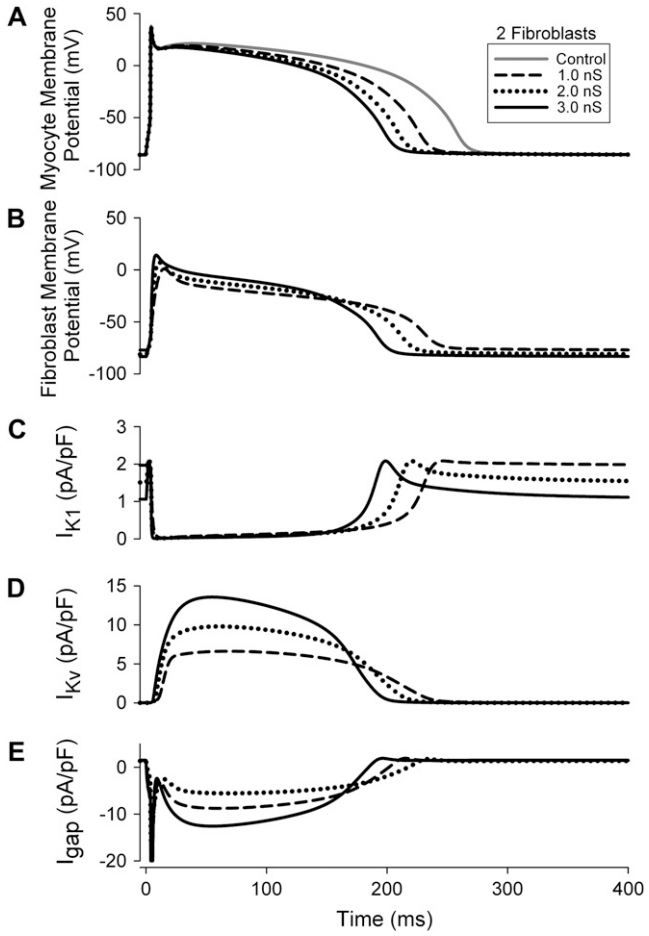

FIGURE 5 Illustration of changes in the waveform of the ventricular action potential (*A*), the fibroblast membrane potential (*B*), I_{K1}, the inwardly-rectifying K^+ current in the fibroblast (*C*), I_{Kv}, the time- and voltage-gated K^+ current in the fibroblast (*D*), and I_{gap}, the gap junction current (*E*) during a ventricular action potential after coupling of the myocyte to two active fibroblasts with a junctional conductance of 1 (*dashed line*), 2 (*dotted line*), or 3 (*solid black line*) nS. The control myocyte action potential is shown as a gray line in *A*.

fibroblast, which activated both K^+ currents that are expressed in it. In addition, as a consequence of coupling, the diastolic potential of each fibroblast was significantly hyperpolarized compared with the membrane potential of the uncoupled fibroblast, which was −49.6 mV. For example, when two or four fibroblasts were coupled to a ventricular myocyte with a junctional conductance of 3 nS, the resting potential of the fibroblasts was −82.7 mV or −82.5 mV, respectively.

Note that each action potential in the myocyte results in a marked change in the fibroblast membrane potential (Figs. 4 *B* and 5 *B*); thus, ventricular activity drives cyclic electrotonic depolarizations and repolarizations in each fibroblast. These electrotonic changes in fibroblast membrane potential are only ~80% of the amplitude of the corresponding action potential in the myocyte, but their durations closely match myocyte APD. As expected, no voltage threshold or regenerative excitability was apparent in any of the fibroblasts.

Figs. 4, *C* and *D*, and 5, *C* and *D*, demonstrate that resistive coupling of one or more fibroblasts to a human ventricular myocyte results in activation of I_{K1} and I_{Kv} in each fibroblast. Since the magnitude of I_{K1} is a quasi-instantaneous function of membrane potential and since the ion transfer relationship for this K^+ current shows marked inward rectification, it is not changed significantly by the shorter APD in the myocyte resulting from coupling to fibroblasts. In contrast, and as shown in Figs. 4 *D* and 5 *D*, the time- and voltage-dependent delayed-rectifier K^+ current, I_{Kv}, in the cardiac fibroblast is strongly dependent on the magnitude and duration of the electrotonic potential of the fibroblast. This results from the strong voltage dependence of activation of this current and the fact that the plateau height of the ventricular action potential is reduced when fibroblasts are coupled to the myocyte. The records in Figs. 4 *E* and 5 *E* illustrate the current flowing through the intercellular gap junctions with increasing number of coupled fibroblasts (Fig. 4) and with increased coupling conductance for a given number of fibroblasts (Fig. 5).

DISCUSSION

Significance of our findings

Our mathematical model provides novel insights into some of the functional consequences of electrotonic coupling between adult ventricular fibroblasts and myocytes. When the fibroblast is considered to consist of a passive resistance in parallel with the membrane capacitance, resistive coupling to a human ventricular myocyte results in relatively small changes in excitability and action potential waveform. In contrast, when formulations for the fibroblast I_{K1} and I_{Kv} currents are included, the height of the plateau phase of the action potential is reduced, and the APD is shortened significantly. Such changes in action potential waveform would be predicted to alter Ca^{2+} transient in the myocyte and, in this way, modulate contraction and left-ventricular pressure development. Previous experiments (11,18) and theoretical work (19) have explored the consequences of the electrophysiological interactions between fibroblasts and myocytes in the context of stretch-induced mechanotransduction, or slow conduction in the ventricle.

Adult ventricular fibroblasts are nonexcitable. We and others have been unable to record voltage-gated Na^+ or L-type Ca^{2+} currents in them (12,13). However, as shown in Figs. 4 and 5, in silico heterocellular coupling induced significant electrotonic depolarizations in each fibroblast in response to action potentials in the coupled myocyte. A similar pattern of responses has been observed previously in myocyte/fibroblast and myocyte/myofibroblast coculture experiments based on cells from neonatal rat hearts (8,9). The physiological consequences of these electrotonic depolarizations of the fibroblast, which occur in response to each ventricular action potential, have not been studied in detail. However, this type of repetitive depolarization of the fibroblast

would be expected to strongly modulate Ca^{2+} homeostasis and excitation-secretion coupling. Thus, it could regulate release of autocrine/paracrine factors and/or procollagen (20,21).

The electrophysiological studies of Rook et al. (7), as well as important findings published by Kohl et al. (5,18), imply that small electrical or mechanical perturbations in the cardiac fibroblast can alter the action potential profile of the myocyte to which fibroblasts are coupled. We have not incorporated any mechanosensitive current into either the myocyte or fibroblast models that represent human ventricle. However, our results suggest that the addition of time- and voltage-sensitive currents, which are activated by depolarization in the fibroblast, can, in turn, significantly affect the excitability, APD, and contractility of the human ventricular myocyte. This possibility needs to be explored in relation to the safety factor or repolarization reserve of the ventricular myocyte (22), or when considering regulation of the dispersion of APD (23).

The work of Gaudesius et al. (8) provides evidence that in addition to having significant effects upon the electrophysiological responses of the myocyte, the fibroblast can function as a conductive element within cocultured systems of neonatal cardiac cells. Although this effect has not been addressed in detail using our model, our computational work and a previous article (19) suggest that cardiac fibroblasts can act as a conductive bridge between myocytes. In this way, fibroblasts can modulate conduction velocity, as well as the action potential waveform in the myocyte.

Resting membrane potential of fibroblasts

There is a paucity of quantitative data on electrophysiological properties of fibroblasts in general, and especially adult cardiac fibroblasts. Our model, described here, of the acutely isolated, adult rat ventricular fibroblast includes four membrane currents: an inwardly-rectifying K^+ current, a time- and voltage-dependent ''delayed-rectifier'' K^+ current, an electrogenic Na^+/K^+-ATPase, and a time-independent ''background'' Na^+ conductance. The magnitude and kinetics of the inwardly rectifying and delayed-rectifier K^+ currents are based directly on our experimental measurements (12,13). The Na^+/K^+-ATPase and the background Na^+ current were introduced to account for K^+ and Na^+ ion homeostasis. The resting membrane potential of the in silico uncoupled fibroblast is −49.6 mV, with an input (slope) resistance of ~6.9 GΩ, between −60 and −80 mV. We previously reported a resting membrane potential of acutely isolated rat ventricular fibroblasts of −58.0 mV, and an apparent input resistance of between ~6 and 11 GΩ (12,13).

The resting membrane potential of our fibroblast model is more negative than some previous reports in the literature. There are at least two reasons why our results may appear to differ from those of others:

1. Kamkin et al. (10) reported a resting membrane potential of −37mV for freshly isolated, mechanically unstressed adult rat atrial fibroblasts, measured using patch-clamp methods. The resting membrane potential of these cells was sensitive to mechanical stress; a stretch of 2–3 μm produced a hyperpolarization to resting membrane potential between −45.0 and −61.0 mV. Gadolinium hyperpolarized these cells to −90 mV. Hyperpolarization was attributed to reduction in the activation of a nonselective cation current. We did not include such a current in our model of rat ventricular fibroblasts, because we have not undertaken experiments similar to those of Kamkin et al. (10) to attempt to identify stretch-sensitive ion channels in our acutely isolated ventricular fibroblasts. If this ion channel is present in our ventricular fibroblasts, it is possible that it is inactivated under our experimental conditions, and hence would not contribute a depolarizing current. In addition, the fibroblasts of Kamkin et al. (10) did not show either inwardly rectifying or voltage-gated delayed-rectifier K^+ currents such as those reported by us in acutely isolated rat ventricular fibroblasts. Lack of hyperpolarizing K^+ currents in rat atrial fibroblasts might account in part for a more positive resting membrane potential than that found for rat ventricular fibroblasts.
2. Rook et al. (7) presented an example of the I-V relation of an isolated, cultured neonatal myofibroblast, which showed a zero-current potential of ~−30 mV, and an apparent input resistance of ~25 GΩ at membrane potentials negative to −20 mV. The apparent resting membrane potential and input resistance of small, isolated cells with high input resistance can be importantly influenced by the membrane seal resistance of the patch electrode. The membrane seal resistance will tend to depolarize the patched cell, due to a current-shunting, or ''voltage-divider'' effect of the seal resistance (24,25). For example, in our model of the ventricular fibroblast, addition of a 10-GΩ ''seal resistance'' to the other membrane currents in the model depolarized the resting membrane potential to −42.3 mV. Even under the excellent experimental conditions of Rook et al. (7), where the patch electrode-membrane seal resistance is high (e.g., >10 GΩ), it is probable that the apparent cell resistance of 25 GΩ of the sample fibroblast is significantly influenced by the patch-pipette seal resistance, and that the true input resistance of the fibroblast is higher, and the true resting membrane potential more negative, than that recorded. In our experiments, we attempted to correct recorded membrane currents for patch electrode seal leakage currents (12), which may account for our more negative estimates of resting membrane potential.

Depolarization of resting membrane potential of fibroblast-coupled myocytes

Previous studies of fibroblast-myocyte interactions using neonatal myocyte-fibroblast coculture models have shown

that the fibroblasts depolarize electrotonically coupled myocytes (e.g., Miragoli et al. (9)). Our simulations also show a depolarizing effect of coupled fibroblasts on resting membrane potential of the ventricular myocytes, although this effect is small and is not readily apparent in Figs. 2–5. Fig. 6 *A* shows the relation between the resting membrane potential of fibroblasts and the coupled myocyte as the number of coupled fibroblasts is increased. The resting membrane potential of the coupled myocyte is increasingly depolarized as the number of fibroblasts increases, but the depolarizing effect is small: even when as many as 10 fibroblasts are coupled to a myocyte, the resting membrane potential of the myocyte is depolarized by only 2.7 mV. The resting membrane potential of the coupled fibroblasts, however, is hyperpolarized by 30.8 mV. Fig. 6 *B* shows the relation between resting membrane potential of fibroblasts and the coupled myocyte as the magnitude of G_{gap} is increased, when the number of fibroblasts is fixed ($n = 2$). Note that in these conditions the resting membrane potential of the coupled fibroblasts is relatively sensitive to G_{gap}, but the resting membrane potential of the coupled myocyte is insensitive to changes in coupling conductance. Although these depolarizing effects are small, they are consistent with the properties of ventricular myocytes in intact myocardium. The resting membrane potential of isolated ventricular myocytes is very similar to the resting membrane potential of myocytes in intact ventricular tissue. If fibroblast-myocyte interactions caused a significant depolarization of the myocytes, a difference between the resting membrane potential of isolated and in situ ventricular myocytes would be expected.

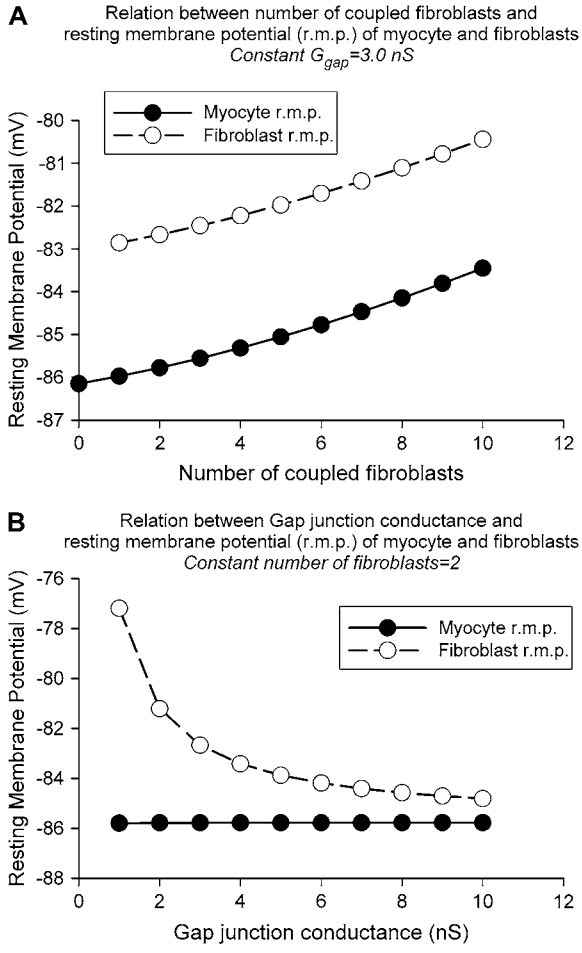

FIGURE 6 Effect of coupling fibroblasts and myocytes on fibroblast and myocyte resting membrane potential.

The very small effect of coupled fibroblasts on resting membrane potential of myocytes in our model calculations appears to disagree with previous results in neonatal cocultured systems (9). However, there are important quantitative differences between myofibroblast-cardiomyocyte interactions in these cocultured systems, and the adult fibroblast-ventricular myocyte interactions that are the focus of our model. The major difference between cocultured neonatal models and our computer model is in the relative sizes of the fibroblast and myocyte. In cocultured systems, the membrane capacitance of myofibroblasts may be large compared with the membrane capacitance of myocytes. For example, we reported that the average capacitance of adult rat cultured myofibroblasts was ~53 pF, compared with ~6 pF for an acutely isolated fibroblast (12). We are unaware of any data for the capacitance of neonatal cardiac myofibroblasts in culture, but it is likely that their capacitance will be comparable to that of neonatal rat cultured myocytes, which range from 9 to 92 pF, depending on the age of donors, culture conditions, and duration (26,27,28). In our model of the adult myocyte-fibroblast interaction, the membrane capacitance of the ventricular myocyte is very much greater than that of the coupled fibroblasts (185 vs. ~6 pF/fibroblast). In addition, there is a much closer match of cardiomyocyte and fibroblast membrane resistances in the cocultured system than in the adult fibroblast-myocyte system. Rook et al. (7) state that the input resistance of myocytes in their cocultures was ~2–10 GΩ at resting membrane potential, compared with up to 30 GΩ for fibroblasts. In our computer model, the membrane resistance of the ventricular myocyte near resting membrane potential is only ~50 MΩ, compared with a fibroblast input resistance of ~6 GΩ. In general, the closer the match between membrane resistances of the coupled fibroblasts and myocytes, the greater the influence of fibroblasts on the myocyte resting membrane potential will be. Hence, a much greater effect of coupled fibroblasts on myocyte behavior would be expected in the cocultured system than in our computer model, where there is a very large mismatch between the magnitude of the membrane capacitance and resistance of the fibroblast and the ventricular myocyte.

In addition to the effects on resting membrane potentials, the relative sizes of coupled fibroblasts and myocytes has important implications for the changes in membrane currents and potential that occur during the myoycte action potential. We have explored this by doing a simulation in which the fibroblast capacitance was increased 10-fold to 60 pF while

the myocyte capacitance was kept at 185 pF; all other parameters (i.e., membrane current densities) were unchanged. Fig. 7 compares ventricular action potential and membrane currents when fibroblasts of 6 pF or 60 pF are coupled to a myoycte (junctional conductance = 3 nS). These data show that there was a much larger effect of large fibroblasts on ventricular action potential and membrane currents, compared with that of the small fibroblasts. There was a significant depolarization of the resting membrane potential of the myocyte when large fibroblasts were coupled. Because of this depolarization there was a large diastolic I_{K1}, and APD was shortened much more when large fibroblasts were coupled. Fig. 8 compares the electrotonic potentials and membrane currents in large and small coupled fibroblasts. Note that there were very large differences in the respective electrotonic potentials and membrane currents between large and small fibroblasts. For example, the resting membrane potential of small fibroblasts was close to the myocyte resting membrane potential, but was very much more depolarized (i.e., much closer to the uncoupled resting membrane potential) for the large fibroblasts. The electrotonic potential in the large fibroblasts during the myocyte action potential was much smaller than that in the small fibroblasts. Membrane currents in the large fibroblasts were also much smaller than the corresponding currents in small fibroblasts: for example, I_{K1} and I_{Kv} were very weakly activated in the large fibroblasts compared with the small. These data make it clear that it is the relative ''loading'' effects of the coupled cells that determine the extent of depolarization of resting membrane potential and changes in myocte action potentials and fibroblast electrotonic potentials that will occur when the cells are coupled together. The relative sizes of myocytes and coupled fibroblasts may also have an important influence on conduction. Miragoli et al. (9) have reported a significant reduction of conduction velocity when strands of cultured myocytes are coupled to cultured myofibroblasts in vitro. This

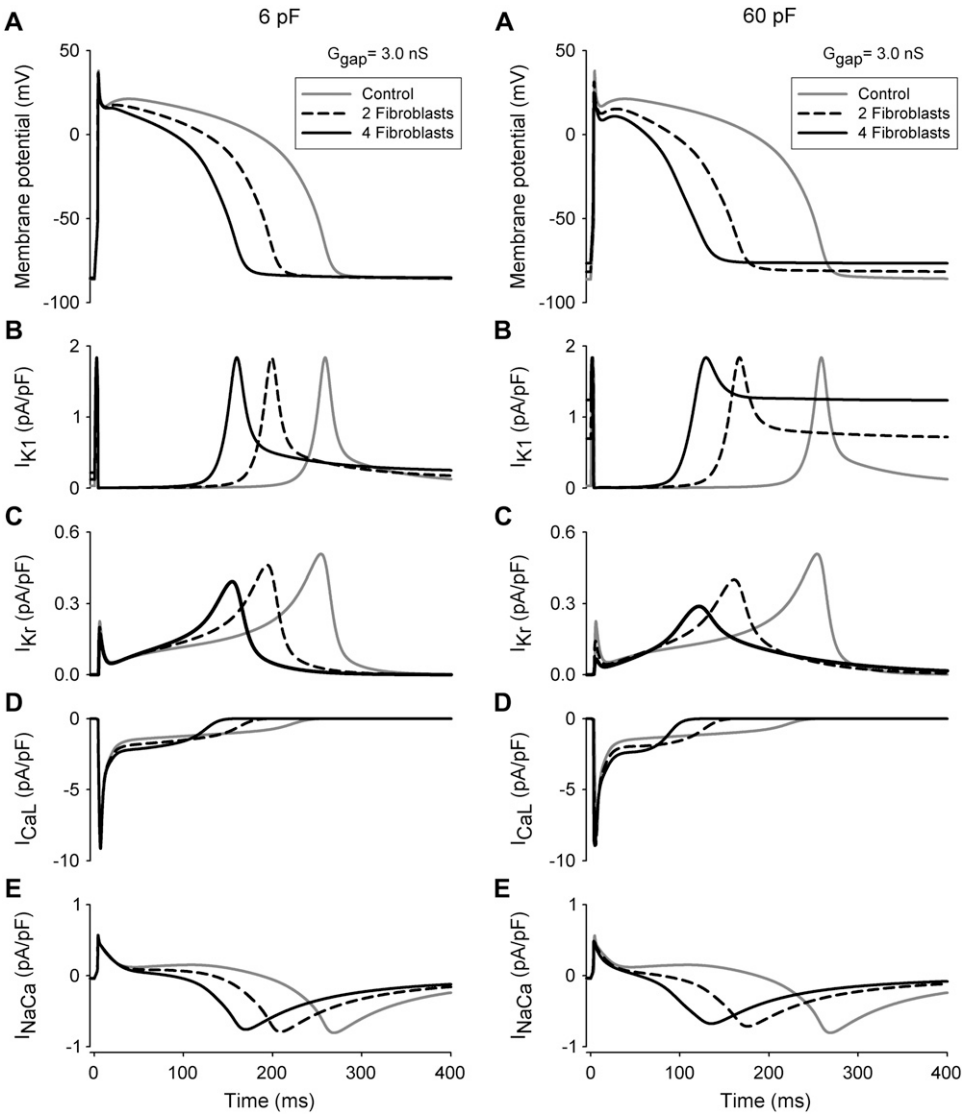

FIGURE 7 Comparison of the effects on myocyte action potential and membrane currents of coupling two or four 6-pF (*left-hand column*) or 60-pF (*right-hand column*) fibroblasts to a 185-pF myocyte. Junctional conductances were fixed at 3 nS. Note the significant depolarization of resting membrane potential of the myocyte when coupled to 60-pF fibroblasts, but not to 6-pF fibroblasts (*A*).

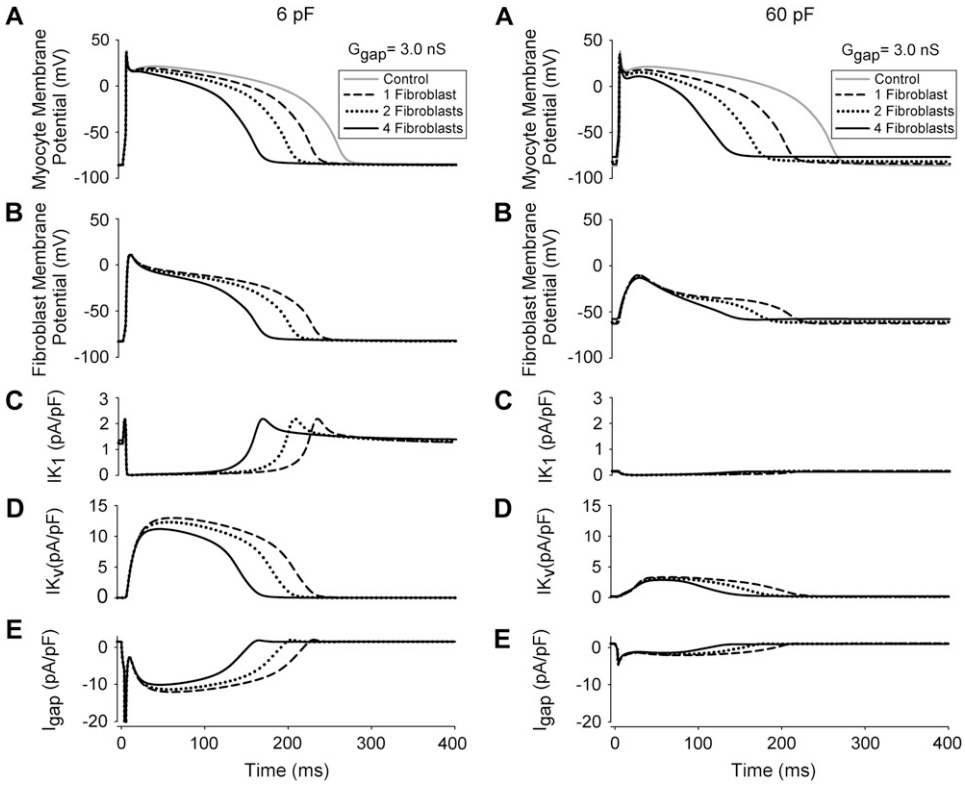

FIGURE 8 Comparison of the effects on fibroblast membrane potential and currents of coupling one, two, or four 6-pF (*left-hand column*) or 60-pF (*right-hand column*) fibroblasts to a 185-pF myocyte. Myocyte membrane potential is shown in Panel *A* of each column. Junctional conductance was fixed at 3 nS. Note that resting membrane potential of the fibroblast is much more negative when the myocyte is coupled to 6-pF fibroblasts than to 60-pF fibroblasts (*B*), even though the uncoupled resting membrane potential of the 6-pF and 60-pF fibroblasts is identical.

may arise as a consequence of the relatively large capacitance of the myofibroblast in cocultured systems.

The study of Kizana et al. (29), in which coupled fibroblasts were shown to alter the spontaneous beat frequency of cardiomyocytes, was carried out with a cocultured neonatal rat model system, where the influence of the coupled myofibroblasts on myocytes would be expected to be much greater than in our adult model system. This experimental model may be more relevant to the SAN node than to fibroblast-myocyte interactions in the mammalian ventricle.

In summary, differences between our computer model and systems of cocultured neonatal myofibroblasts and myocytes reflect quantitative, rather than qualitative, differences between the two situations. It is therefore not surprising that our computer model of the adult myocyte-fibroblast interaction shows much smaller effects on the resting membrane potential of the myocytes than is observed in cultured neonatal systems. We suggest that neonatal cultured model systems may exaggerate the effects of fibroblast-myocyte interactions and thus may not accurately reflect adult fibroblast-myocyte interactions that we are attempting to model. Instead, they may be more relevant to the embryonic or neonatal heart, or perhaps to supraventricular syncytial components of the myocardium where microfibrosis is well known to alter excitability and impulse conduction (30). On the other hand, our model may underestimate the effects of coupled fibroblasts in the in situ myocardium. Structural studies of fibroblast-myocyte interactions in cardiac tissue have identical extended fibroblast ''processes'' in close association with the myocytes (4). These finger-like processes appear to be lost in the isolation procedure, possibly making the isolated fibroblasts significantly smaller than they are in situ.

Consequences of fibroblast-myocyte interactions for ventricular electrophysiology and excitation-contraction coupling

Our simulations suggest that resistive coupling of a myocyte with two to four fibroblasts, each of which expresses K^+ currents, can reduce the height of the action potential plateau and shorten APD in human ventricle. Although these changes may have relatively few consequences for normal conduction and/or excitation-contraction coupling under control conditions, in the setting of reduced ''repolarization reserve'', they may become significant (22). For example, in cardiac tissue exhibiting fibrosis, the number of fibroblasts per atrial or ventricular myocyte increases (31,32). Repolarization reserve of the myocyte is also reduced in acute ischaemia, in which the ventricular myocyte depolarizes and extracellular $[K^+]$ increases (33–35). Under these ischemic conditions, Na^+ current is reduced due to depolarization of the resting potential (36), and the background inwardly-rectifying K^+ current is changed in a complex fashion (35,37). In this setting, electrotonic coupling to a population of fibroblasts is predicted to further compromise myocyte action potential properties and may result in conduction block (simulations not shown).

Our simulations indicate that coupling of fibroblasts to ventricular myocytes tends to shorten the myocyte APD.

This may have significant implications for the development of spatial heterogeneities within the myocardium: given that there is spatial variation in fibroblast density (4), the number of fibroblasts coupled to each myocyte and the resultant shortening of APD may also be variable. This heterogeneity could augment the intrinsic transmural heterogeneity due to altered ion channel expression in the epicardium, midmyocardium, and endocardium. Our simulations consider the effect of two and four fibroblasts coupled to a single myocyte. We acknowledge that it is likely that when cardiac myocytes are also coupled with other myocytes, the effect of the fibroblasts on myocyte action potential waveform may not be as pronounced.

Fibroblast-myocyte coupling and Regenerative Medicine

The recognition and description of microanatomical and functional coupling between cardiac myocytes and fibroblasts have provided opportunities for delivering ion channels or connexons to ventricular tissue using genetically engineered constructs transfected into fibroblasts. For example, Feld et al. (38) have attempted to modulate ventricular excitability and diastolic membrane potential by introducing populations of fibroblasts transfected with K^+ channels into the ventricular myocardium. Based on a somewhat similar rationale, fibroblasts have been targeted to the canine atrioventricular node and then stimulated with TGF-β1 in an effort to augment atrioventricular node conduction (39). In addition, Kizana et al (40) have transfected dermal fibroblasts with Cx43 in an effort to enhance intercellular coupling in a myotube preparation as proof of principle for planned experiments in mammalian ventricular syncytia.

Limitations/planned studies

Our computational work has provided a number of novel insights into the consequences of electrotonic interactions between fibroblasts and human ventricular myocytes. In addition, this approach offers a very useful means for integrating and illustrating experimental data. Nevertheless, the limitations of our work need to be clearly recognized:

1. The values for gap-junctional conductances between fibroblasts and myocytes in the adult ventricle are not known with certainty.
2. The chosen fibroblast/myocyte ratio is only an approximation (3,31,32). It will be necessary to refine our model as these data become available.
3. Although the ten Tusscher model of the human ventricle (14) is self-consistent and robust (see Methods), it will need to continue to evolve as the electrophysiological data on the human ventricular myocyte is published.
4. There is some concern and uncertainty regarding the validity of using cell-culture procedures to study cell-cell interactions; for example, Levitan et al. (41) have reported very rapid changes in sarcolemmal ion channel density after alterations in culture density or cell-cell contact. In addition, there are reports that cell culture or coculture can result in dedifferentiation in cardiac myocytes and fibroblasts (42,43).

Because of these limitations, it will be important to attempt to identify fibroblast myocyte interactions in intact or freshly isolated ventricular tissue, perhaps by using voltage-sensitive dye methods (44). This type of data will also provide a basis for adapting our 1-D model to explore excitability, action potential waveform, and electrotonic potentials in a 2-D syncytium consisting of various combinations of myocytes and fibroblasts, under both physiological and pathophysiological conditions.

SUPPLEMENTARY MATERIAL

An online supplement to this article can be found by visiting BJ Online at http://www.biophysj.org.

This work was supported by grants from the Canadian Institutes of Health Research (W.R.G.), the Heart and Stroke Foundation of Canada (W.R.G. and L.C.), the Alberta Heritage Foundation for Medical Research (W.R.G. and L.C.), and the Research Chair sponsored by the Heart and Stroke Foundation of Alberta and the Northwest Territories (W.R.G.).

REFERENCES

1. Zak, R. 1973. Cell proliferation during cardiac growth. *Am. J. Cardiol.* 31:211–219.
2. Goldsmith, E. C., A. Hoffman, M. O. Morales, J. D. Potts, R. L. Price, A. McFadden, M. Rice, and T. K. Borg. 2004. Organization of fibroblasts in the heart. *Dev. Dyn.* 230:787–794.
3. Camelliti, P., C. R. Green, I. LeGries, and P. Kohl. 2004. Fibroblast network in rabbit sinoatrial node: structural and functional identification of homogeneous and heterogeneous cell coupling. *Circ. Res.* 94: 828–835.
4. Camelliti, P., T. K. Borg, and P. Kohl. 2005. Structural and functional characterization of cardiac fibroblasts. *Cardiovasc. Res.* 65:40–51.
5. Kohl, P., P. Camelliti, F. L. Burton, G. L. Smith. 2005. Electrical coupling of fibroblasts and myocytes: relevance for cardiac propagation. *J. Electrocardiol.* 38:45–50.
6. Hooks, D. A., K. A. Tomlinson, S. G. Marsdan, I. J. LeGrice, B. H. Smaill, A. J. Pullan, and P. J. Hunter. 2002. Cardiac microstructure: implications for electrical propagation and defibrillation in the heart. *Circ. Res.* 91:331–338.
7. Rook, M. B., A. C. G. van Ginneken, B. De Jonge, A. Elaoumari, D. Gros, and H. J. Jongsma. 1992. Differences in gap junction channels between cardiac myocytes, fibroblasts, and heterologous pairs. *Am. J. Physiol.* 263:C959–C977.
8. Gaudesius, G., M. Miragoli, S. P. Thomas, and S. Rohr. 2003. Coupling of cardiac electrical activity over extended distances by fibroblasts of cardiac origin. *Circ. Res.* 93:421–428.
9. Miragoli, M., G. Gaudesius, and S. Rohr. 2006. Electrotonic modulation of cardiac impulse conduction by myofibroblasts. *Circ. Res.* 98: 801–810.
10. Kamkin, A., I. Kiseleva, and G. Isenberg. 2003. Activation and inactivation of a non-selective cation conductance by local mechanical deformation of acutely isolated cardiac fibroblasts. *Cardiovasc. Res.* 57:793–803.

11. Kamkin, A., I. Kiseleva, I. Lozinsky, and H. Scholz. 2005. Electrical interaction of mechanosensitive fibroblasts and myocytes in the heart. *Basic Res. Cardiol.* 100:337–345.

12. Chilton, L., S. Ohya, D. Freed, E. George, V. Drobic, Y. Shibukawa, K. A. MacCannell, Y. Imaizumi, R. B. Clark, I. M. C. Dixon, and W. R. Giles. 2005. K^+ currents regulate the resting membrane potential, proliferation, and contractile responses in ventricular fibroblasts and myofibroblasts. *Am. J. Physiol.* 288:H2931–H2939.

13. Shibukawa, Y., E. L. Chilton, K. A. MacCannell, R. B. Clark, and W. R. Giles. 2005. K^+ currents activated by depolarization in cardiac fibroblasts. *Biophys. J.* 88:3924–3935.

14. ten Tusscher, K. H. W. J., D. Noble, P. J. Noble, and A. V. Paniflov. 2004. A model for human ventricular tissue. *Am. J. Physiol.* 286: H1573–H1589.

15. Priebe, L., and D. J. Beuckelmann. 1998. Simulation study of cellular electric properties in heart failure. *Circ. Res.* 82:1206–1223.

16. ten Tusscher, K. H. W. J., O. Bernus, R. Hren, and A. V. Paniflov. 2006. Comparison of electrophysiological models for human ventricular cells and tissues. *Prog. Biophys. Mole. Biol.* 90:326–345.

17. Nygren, A., C. Fiset, L. Firek, J. W. Clark, D. S. Lindblad, R. B. Clark, and W. R. Giles. 1998. A mathematical model of an adult human atrial cell: the role of K^+ currents in repolarization. *Circ. Res.* 82:63–81.

18. Kohl, P., A. Kamkin, I. Kiseleva, and D. Noble. 1994. Mechanosensitive fibroblasts in the sino-atrial node of rat heart: interaction with cardiomyocytes and possible role. *Exp. Physiol.* 79:943–956.

19. Vásquez, C., R. A. Siddiqui, A. P. Moreno, and E. J. Berbari. 2002. A fibroblast-myocyte model which accounts for slow conduction and fractionated electrograms in infarct border zones. *Comp. Cardiol.* 29: 245–248.

20. Isenberg, G. 2004. Ca^{2+} control of transcription: can we extrapolate signaling cascades from neurons to vascular smooth muscle cells? *Circ. Res.* 94:1276–1278.

21. MacKenna, D., S. R. Summerour, and F. J. Villarreal. 2000. Role of mechanical factors in modulating cardiac fibroblast function and extracellular matrix synthesis. *Cardiovasc. Res.* 46:257–263.

22. Fink, M., W. Giles, and D. Noble. 2006. Contributions of inwardly rectifying K^+ currents to repolarization assessed using mathematical models of human ventricular myocytes. *Phil. Trans. A. Math. Phys. Eng. Sci.* 364:1207–1222.

23. Burton, F. L., and S. M. Cobbe. 1998. Effect of sustained stretch on dispersion of ventricular fibrillation intervals in normal rabbit hearts. *Cardiovasc. Res.* 39:351–359.

24. Fenwick, E. M., A. Marty, and E. Neher. 1982. A patch-clamp study of bovine chromaffin cells and of their sensitivity to acetylcholine. *J. Physiol.* 331:577–597.

25. Mason, M. J., A. K. Simpson, M. P. Mahaut-Smith, and H. P. C. Robinson. 2005. The interpretation of current-clamp recordings in the cell-attached patch-clamp configuration. *Biophys. J.* 88:739–750.

26. Wickenden, A. D., R. Kaprielian, T. G. Parker, O. T. Jones, and P. H. Backx. 1997. Effects of development and thyroid hormone on K^+ currents and K^+ channel gene expression in rat ventricle. *J. Physiol.* 504:271–286.

27. Guo, W., K. Kamiya, and J. Toyama. 1996. Modulated expression of transient outward current in cultured neonatal rat ventricular myocytes: comparison with development in situ. *Cardiovasc. Res.* 32:524–533.

28. Kilborn, M. J., and D. Fedida. 1990. A study of the developmental changes in outward currents of rat ventricular myocytes. *J Phsyiol.* 430:37–60.

29. Kizana, E., S. L. Ginn, C. M. Smyth, S. P. Thomas, D. G. Allen, D. L. Ross, and I. E. Alexander. 2006. Fibroblasts modulate cardiomyocyte excitability: implications for cardiac gene therapy. *Gene Ther.* 13:1611–1615.

30. Spach, M. S., and J. P. Boineau. 1997. Microfibrosis produces electrical load variations due to loss of side-to-side cell connections: a major mechanism of structural heart disease arrhythmias. *PACE.* 20:397–413.

31. Nag, A. 1980. Study of non-muscle cells of the adult mammalian heart; a fine structural analysis and distribution. *Cytobios.* 28:41–61.

32. Baudino, T., W. Carver, W. R. Giles, and T. K. Borg. 2006. Cardiac fibroblasts: friend or foe. *Am. J. Physiol.* 291:H1015–H1026.

33. Kleber, A. G., J. Fleischhauer, and W. E. Cascio. 1995. Ischemia-induced propagation failure in the heart. *In* Cardiac Electrophysiology: From Cell to Bedside, 2nd ed. D. Zipes and J. Jalife, editors. Saunders, Philadelphia. 174–182.

34. Carmeliet, E. 1999. Cardiac ionic currents and acute ischemia: from channels to arrhythmias. *Physiol. Rev.* 79:917–1017.

35. Nygren, A., I. Baczko, and W. Giles. 2006. Measurements of electrophysiological effects of components of acute ischaemia in Langendorff-perfused rat hearts using voltage-sensitive dye mapping. *J. Cardiovasc. Electrophysiol.* 17:S113–S123.

36. Nerbonne, J. M., and R. S. Kass. 2005. Molecular physiology of cardiac repolarization. *Physiol. Rev.* 85:1205–1253.

37. Diaz, R. J., C. Zobel, H. C. Cho, M. Batthish, A. Hinek, P. H. Backx, and G. J. Wilson. 2004. Selective inhibition of inward rectifier K^+ channels (Kir2.1 or Kir2.2) abolishes protection by ischemic preconditioning in rabbit ventricular cardiomyocytes. *Circ. Res.* 95:325–332.

38. Feld, Y., M. Melamed-Frank, I. Kehat, D. Tal, S. Marom, and L. Gepstein. 2002. Electrophysiological modulation of cardiomyocytic tissue by transfected fibroblasts expressing potassium channels: a novel strategy to manipulate excitability. *Circulation.* 105:522–529.

39. Bunch, T. J., S. Mahapatra, G. K. Bruce, S. B. Johnson, D. V. Miller, B. D. Horne, X.-L. Wang, H.-C. Lee, N. M. Caplice, and D. L. Packer. 2006. Impact of transforming growth factor-β1 on atrioventricular node conduction modification by injected autologous fibroblasts in the canine heart. *Circulation.* 113:2485–2494.

40. Kizana, E., S. L. Ginn, D. G. Allen, D. L. Ross, and I. E. Alexander. 2005. Fibroblasts can be genetically modified to produce excitable cells capable of electrical coupling. *Circulation.* 111:394–398.

41. Hershman, K. M., and E. S. Levitan. 1998. Cell-cell contact between adult rat cardiac myocytes regulates Kv1.5 and Kv4.2 K^+ channel mRNA expression. *Am. J. Physiol.* 275:C1473–C1480.

42. Driesen, R. B., G. D. Dispersyn, and F. K. Verhayen. 2005. Partial cell fusion: a newly recognized type of communication between dedifferentiating cardiomyocytes and fibroblasts. *Cardiovasc. Res.* 68:1–2.

43. Dispersyn, G. D., E. Geuens, L. Ver Donck, F. C. S. Ramaekers, and M. Borgers. 2001. Adult rabbit cardiomyocytes undergo hibernation-like dedifferentiation when co-cultured with cardiac fibroblasts. *Cardiovasc. Res.* 51:230–240.

44. Akar, F. G., B. J. Roth, and D. S. Rosenbaum. 2001. Optical measurement of cell-to-cell coupling in intact heart using subthreshold electrical stimulation. *Am. J. Physiol.* 281:H533–H542.